

Luminosity and beam-beam tune shifts with crossing angle and hourglass effects in e^+e^- colliders

Tanaji Sen
Accelerator Division, Fermilab
Batavia, IL 60510

Abstract

We develop theoretical expressions for the luminosity and beam-beam tune shifts in the presence of both a crossing angle and hourglass effects for the present and next generation of symmetric e^+e^- colliders. The theory is applied to the design of the Fermilab site filler Higgs factory and to the FCC-ee collider.

1 Introduction

Introducing a crossing angle reduces both the luminosity and beam-beam tune shifts if no optics changes are made. The lowered beam-beam tune shifts however allow the possibility of further reducing the beta functions at the IP to increase the luminosity while keeping the beam-beam tune shifts within allowed limits. Specifically, in an e^+e^- collider where $\beta_y^* \ll \beta_x^*$, a crossing angle in the horizontal plane allows a scheme where β_x^* is reduced sufficiently to increase the luminosity beyond values without a crossing angle. This has been investigated in recent designs of colliders such as Super KEKB [1], FCC-ee [2] etc. We include both the crossing angle and the hourglass effects on the luminosity and the beam-beam tune shifts. Analytic expressions for the combined effects do not appear to be available in the literature; instead they are approximated as acting independently. The only assumption in our treatment below is that of symmetric interaction region optics for the electrons and positrons so that the bunch sizes in all three dimensions are the same in both beams. After developing exact general expressions, we consider several limiting cases and show that they reduce to known forms where applicable. The purpose of this paper is to find appropriate combinations of the crossing angle and (β_x^*, β_y^*) which maximize the luminosity while restricting the beam-beam tune shifts to tolerable values.

We first apply the theory to the very preliminary design of a Higgs factory at Fermilab, called a site filler, and find parameters that increase the luminosity with a non-zero crossing angle. Next we apply the theory to the FCC-ee collider whose design is considerably more mature. We find that the luminosity in this design can also be increased with changes in the crossing angle and β_x^* .

2 Luminosity change with a crossing angle and hourglass effect

The relativistically invariant luminosity per bunch and unit time is [3]

$$\mathcal{L} = K f_{rev} N_+ N_- \int_{-\infty}^{\infty} \int_{-\infty}^{\infty} \int_{-\infty}^{\infty} \int_{-\infty}^{\infty} ds dt dx dy \rho_-(xy, s - ct) \rho_+(x, y, s - ct) \quad (2.1)$$

(N_-, ρ_-) , (N_+, ρ_+) are the (bunch intensities, three dimensional densities) of the electrons and positrons respectively and K is a kinematic factor

$$K = \sqrt{(\mathbf{v}_+ - \mathbf{v}_-)^2 - \frac{(\mathbf{v}_+ \times \mathbf{v}_-)^2}{c^2}} \quad (2.2)$$

We assume that the electrons move along the positive s direction and the positrons in the opposite direction. When the beams cross in the horizontal plane at a full angle of θ_C , the coordinates in the two beam frames are

$$\begin{aligned} x_- &= C_C x - S_C s, & s_- &= C_C s + S_C x \\ x_+ &= -C_C x - S_C s, & s_+ &= -C_C s + S_C x \end{aligned} \quad (2.3)$$

where (x, s) are the coordinates in the laboratory frame, $C_C = \cos(\theta_C/2)$, $S_C = \sin(\theta_C/2)$. The transverse velocities are orders of magnitude smaller than the longitudinal velocity ($\simeq c$), so the only velocity components are the projections of the longitudinal velocity,

$$\begin{aligned} \mathbf{v}_- &\equiv \frac{d}{dt}(x_- \hat{x} + 0 \hat{y} + s_- \hat{z}) = (-S_C \hat{x} + 0 \hat{y} + C_C \hat{z})c \\ \mathbf{v}_+ &\equiv \frac{d}{dt}(x_+ \hat{x} + 0 \hat{y} + s_+ \hat{z}) = (-S_C \hat{x} + 0 \hat{y} - C_C \hat{z})c \\ (\mathbf{v}_- - \mathbf{v}_+)^2 &= (0 \hat{x} + 0 \hat{y} + 2C_C \hat{z})^2 c^2 = 4C_C^2 c^2 \\ (\mathbf{v}_+ \times \mathbf{v}_-) &= (0 \hat{x} + 2S_C C_C \hat{y} + 0 \hat{z})c^2 \end{aligned}$$

where $\hat{x}, \hat{y}, \hat{z}$ are unit vectors. Hence the kinematic factor is

$$K = c \sqrt{4C_C^2 - 4S_C^2 C_C^2} = 2c C_C^2 \quad (2.4)$$

The normalized density of the electron and positron bunches are

$$\rho_- = \frac{1}{(2\pi)^{3/2} \sigma_{x-} \sigma_{y-} \sigma_{s-}} \exp \left[-\frac{(C_C x - S_C s)^2}{2\sigma_{x-}^2} - \frac{y^2}{2\sigma_{y-}^2} - \frac{(C_C s + S_C x - ct)^2}{2\sigma_{s-}^2} \right] \quad (2.5)$$

$$\rho_+ = \frac{1}{(2\pi)^{3/2} \sigma_{x+} \sigma_{y+} \sigma_{s+}} \exp \left[-\frac{(-C_C x - S_C s)^2}{2\sigma_{x+}^2} - \frac{y^2}{2\sigma_{y+}^2} - \frac{(S_C x - C_C s - ct)^2}{2\sigma_{s+}^2} \right] \quad (2.6)$$

We assume that the bunches are symmetric at the IP so that the beam sizes in all 3 dimensions are matched, i.e.

$$\sigma_{x+}^* = \sigma_{x-}^*, \quad \sigma_{y+}^* = \sigma_{y-}^*, \quad \sigma_{s+} = \sigma_{s-} = \sigma_s \quad (2.7)$$

This assumption is true for equal high energy colliders that we consider but could be dropped to consider the more general case of asymmetric colliders. We ignore perturbative effects such as a non-zero dispersion or transverse offsets at the IP.

The beta functions depend only on the longitudinal coordinate s in the lab frame, they do not depend on the coordinates in the beam frames. Thus

$$\sigma_{x-}(s) = \sigma_{x+}(s) = \sigma_x(s) = \sqrt{\epsilon_x(\beta_x^* + \frac{s^2}{\beta_x^*})} = \sigma_x^* \sqrt{1 + \frac{s^2}{\beta_x^{*,2}}} \quad (2.8)$$

$$\sigma_{y-}(s) = \sigma_{y+}(s) = \sigma_y(s) = \sigma_y^* \sqrt{1 + \frac{s^2}{\beta_y^{*,2}}} \quad (2.9)$$

Putting all the factors for the luminosity

$$\begin{aligned} \mathcal{L} = & \frac{2cf_{rev}N_+N_-C_C^2}{(2\pi)^3} \int_{-\infty}^{\infty} \int_{-\infty}^{\infty} \int_{-\infty}^{\infty} \int_{-\infty}^{\infty} ds dt dx dy \frac{1}{\sigma_x(s)^2 \sigma_y(s)^2 \sigma_s^2} \exp\left[-\frac{(C_C x - S_C s)^2}{2\sigma_x^2}\right] \\ & \exp\left[-\frac{y^2}{2\sigma_y^2}\right] \exp\left[-\frac{(C_C s + S_C x - ct)^2}{2\sigma_s^2}\right] \exp\left[-\frac{(-C_C x - S_C s)^2}{2\sigma_x^2}\right] \exp\left[-\frac{y^2}{2\sigma_y^2}\right] \\ & \exp\left[-\frac{(C_C s - S_C x + ct)^2}{2\sigma_s^2}\right] \end{aligned}$$

The integrations over t, y, x are straightforward. The last integration over s is

$$\begin{aligned} & \int_{-\infty}^{\infty} \frac{ds}{\sigma_s} \frac{1}{\sqrt{(1 + \frac{s^2}{\beta_x^{*,2}})(1 + \frac{s^2}{\beta_y^{*,2}})}} \exp\left[-\frac{C_C^2 s^2}{\sigma_s^2} - \frac{S_C^2 s^2}{\sigma_x^2}\right] \\ = & \int_{-\infty}^{\infty} du \exp\left[-C_C u^2 (1 + T_C^2 \frac{\sigma_s^2 / \sigma_x^{*2}}{1 + u^2 / (u_x^2)})\right] \frac{1}{\sqrt{(1 + \frac{u^2}{u_x^2})(1 + \frac{u^2}{u_y^2})}} \end{aligned}$$

where we defined

$$u = \frac{s}{\sigma_s}, \quad u_x = \frac{\beta_x^*}{\sigma_s}, \quad u_y = \frac{\beta_y^*}{\sigma_s} \quad T_C = \tan(\theta_C/2) \quad (2.10)$$

Thus the general expression for the luminosity per bunch is

$$\mathcal{L} = \frac{f_{rev}N_+N_-C_C}{4\pi^{3/2}\sigma_x^*\sigma_y^*} \int_{-\infty}^{\infty} du \exp\left[-C_C^2 u^2 (1 + T_C^2 \frac{\sigma_s^2 / \sigma_x^{*2}}{1 + u^2 / (u_x^2)})\right] \frac{1}{\sqrt{(1 + \frac{u^2}{u_x^2})(1 + \frac{u^2}{u_y^2})}} \quad (2.11)$$

and the general correction factor is

$$\begin{aligned} R_L & \equiv \frac{\mathcal{L}}{\mathcal{L}_l} \\ & = \frac{C_C}{\sqrt{\pi}} \int_{-\infty}^{\infty} du \exp\left[-\cos^2(\theta_C/2) u^2 (1 + \tan^2(\theta_C/2) \frac{\sigma_s^2 / \sigma_x^{*2}}{1 + u^2 / (u_x^2)})\right] \frac{1}{\sqrt{(1 + \frac{u^2}{u_x^2})(1 + \frac{u^2}{u_y^2})}} \end{aligned} \quad (2.12)$$

Limiting cases

1. No crossing angle or hourglass

Setting $C_C = 1, T_C = 0$ and $u_x, u_y \rightarrow \infty$, we have

$$\mathcal{L} = \frac{f_{rev} N_+ N_-}{4\pi^{3/2} \sigma_x^* \sigma_y^*} \int_{-\infty}^{\infty} du \exp[-u^2] = \frac{f_{rev} N_+ N_-}{4\pi \sigma_x^* \sigma_y^*} \quad (2.13)$$

the standard expression for the nominal luminosity.

2. Only the hourglass effect, no crossing angle

$$\mathcal{L} = \frac{f_{rev} N_+ N_-}{4\pi^{3/2} \sigma_x^* \sigma_y^*} \int_{-\infty}^{\infty} du \exp[-u^2] \frac{1}{\sqrt{(1 + \frac{u^2}{u_x^2})(1 + \frac{u^2}{u_y^2})}} \quad (2.14)$$

Hence the luminosity correction factor is

$$R_L \equiv \frac{\mathcal{L}}{\mathcal{L}_l} = \frac{1}{\sqrt{\pi}} \int_{-\infty}^{\infty} du \exp[-u^2] \frac{1}{\sqrt{(1 + \frac{u^2}{u_x^2})(1 + \frac{u^2}{u_y^2})}} \quad (2.15)$$

which agrees with the expression Eq.(2.7) in [4].

3. Only the crossing angle, no hourglass effect

In the limit that $\beta_x^*, \beta_y^* \gg \sigma_z^*$, there is very little variation in the transverse sizes across the bunch length. In this limit $(t_x^2, t_y^2 \gg 1$. The dominant contributions to the integral come from the regions close to $t = 0$ because of the exponential factor. In this limit we can assume $(t/t_x)^2, (t/t_y)^2 \ll 1$ and the luminosity is

$$\begin{aligned} \mathcal{L} &= \frac{f_{rev} N_+ N_- C_C}{4\pi^{3/2} \sigma_x^* \sigma_y^*} \int_{-\infty}^{\infty} du \exp[-C_C^2 u^2 (1 + T_C^2 \frac{\sigma_s^2}{\sigma_x^{*2}})] \\ &= \frac{f_{rev} N_+ N_- C_C}{4\pi^{3/2} \sigma_x^* \sigma_y^*} \frac{\sqrt{\pi}}{C_C \sqrt{(1 + T_C^2 \frac{\sigma_s^2}{\sigma_x^{*2}})}} \end{aligned} \quad (2.16)$$

Hence the luminosity correction factor is

$$R_L = \frac{1}{\sqrt{(1 + T_C^2 \frac{\sigma_s^2}{\sigma_x^{*2}})}} \quad (2.17)$$

This is the standard correction factor for the crossing angle.

4. Flat bunch

In this limit, $\sigma_x^* \gg \sigma_y^*$. Since the equilibrium emittances obey $\epsilon_x \gg \epsilon_y$, this is easily satisfied if $\beta_x^* \gg \beta_y^*$, which typically is the case. In this limit we drop all terms with u_x from Eq.(2.11)

$$\mathcal{L} = \frac{f_{rev} N_+ N_- C_C}{4\pi^{3/2} \sigma_x^* \sigma_y^*} \int_{-\infty}^{\infty} du \exp[-C_C^2 u^2 (1 + T_C^2 \frac{\sigma_s^2}{\sigma_x^{*2}})] \frac{1}{\sqrt{(1 + \frac{u^2}{u_y^2})}} \quad (2.18)$$

The luminosity correction factor is

$$R_{flat} = \frac{C_C}{\sqrt{\pi}} \int_{-\infty}^{\infty} du \exp[-C_C^2 u^2 (1 + T_C^2 \frac{\sigma_s^2}{\sigma_x^{*2}})] \frac{1}{\sqrt{(1 + \frac{u^2}{u_y^2})}} \quad (2.19)$$

$$= \frac{C_C}{\sqrt{\pi}} u_Y \exp[\frac{1}{2} b^2 u_y^2] K_0(\frac{1}{2} b^2 u_y^2) \quad (2.20)$$

where

$$b^2 = C_C^2 [1 + T_C^2 \frac{\sigma_z^2}{\sigma_x^{*2}}] \geq 0 \quad (2.21)$$

and K_0 is a Bessel function. There is a similar expression Eq. (2) in [5].

In the absence of a crossing angle so that $C_C = 1, T_C = 0$, we have $b = 1$ and Eq. 2.20 is the same as Eq. (2.12) in Furman.

3 Beam-beam tune shifts

The beam-beam potential for electrons interacting with a positron bunch which has a longitudinally Gaussian density is

$$U(x, y) = \frac{N_+ r_e}{\gamma_e} \int \frac{\exp[-s^2/(2\sigma_s^2)]}{\sqrt{2\pi}\sigma_s} ds \int_0^\infty dq \frac{1}{(2\sigma_x(s)^2 + q)^{1/2} (2\sigma_y(s)^2 + q)^{1/2}} \left\{ 1 - \exp\left[-\frac{x^2}{2\sigma_x(s)^2 + q} - \frac{y^2}{2\sigma_y(s)^2 + q}\right] \right\} \quad (3.1)$$

where the parameters are those of the positron bunch. The potential for electrons interacting with positrons at a full crossing angle θ_C can be found by replacing

$$x \rightarrow C_C x - S_C s, \quad s \rightarrow C_C s + S_C x \quad (3.2)$$

The amplitude dependent beam-beam tune shifts can be obtained from the second derivatives of the potential as

$$\Delta\nu_x(x, y) = -\frac{\beta_x^* N_+ r_e}{4\pi\gamma_e} \frac{\partial^2 U}{\partial x^2}, \quad \Delta\nu_y(x, y) = -\frac{\beta_y^* N_+ r_e}{4\pi\gamma_e} \frac{\partial^2 U}{\partial y^2} \quad (3.3)$$

The beam-beam tune shift parameters are the values of the tune shifts at the origin, i.e.

$$\xi_x = \Delta\nu_x(0, 0), \quad \xi_y = \Delta\nu_y(0, 0) \quad (3.4)$$

Substituting the rotated forms in Eq.(3.2) into the potential, taking the derivatives, evaluat-

ing the terms at the origin and leads to

$$\begin{aligned} \xi_x = & \frac{\beta_x^* N_+ r_e}{2\pi\gamma_e} \int_0^\infty \frac{ds}{\sqrt{2\pi}\sigma_s} \int_0^\infty dq \, 2 \frac{\exp[-\frac{s^2 C_C^2}{(2\sigma_s^2)} - \frac{(s^2 S_C^2)}{(q+2\sigma_x^2(s))}]}{\sqrt{(q+2\sigma_x^2(s))^3 (q+2\sigma_y^2(s))}} \\ & \times C_C^2 \left\{ 1 + 2s^2 S_C^2 \left[\frac{1}{\sigma_s^2} - \frac{1}{q+2\sigma_x^2(s)} \right] \right\} \\ & - \frac{\exp[-\frac{s^2 C_C^2}{2\sigma_s^2}] \left(1 - \exp[-\frac{s^2 S_C^2}{q+2\sigma_x^2(s)}] \right)}{\sigma_s^2 \sqrt{(q+2\sigma_x^2(s))(q+2\sigma_y^2(s))}} S_C^2 \left[1 - \frac{s^2 C_C^2}{\sigma_s^2} \right] \end{aligned} \quad (3.5)$$

$$\xi_y = \frac{\beta_y^* N_+ r_e}{2\pi\gamma_e} \int_{-\infty}^\infty \frac{ds}{\sqrt{2\pi}\sigma_s} \int_0^\infty dq \frac{2 \exp\left(-\frac{t^2 S_C^2 \sigma_s^2}{q+2\sigma_x^2} - \frac{t^2 C_C^2}{2}\right)}{(q+2\sigma_y^2) \sqrt{(q+2\sigma_x^2)(q+2\sigma_y^2)}} \quad (3.6)$$

The different integrations over s cannot all be done analytically, so the 2D integrations have to be done numerically. Transform to dimensionless variables (u, t) and define other dimensionless variables

$$t = \frac{s}{\sigma_s}, \quad t_x = \frac{\beta_x^*}{\sigma_s}, \quad t_y = \frac{\beta_y^*}{\sigma_s} \quad (3.7)$$

$$u = \frac{2\sigma_x^{*,2}}{q+2\sigma_x^{*,2}} \Rightarrow q = 2\sigma_x^{*,2} \left(\frac{1}{u} - 1 \right); \quad 0 \leq u \leq 1 \quad (3.8)$$

$$\Rightarrow \sigma_x(t) = \sigma_x^* \sqrt{1 + \frac{s^2}{\beta_x^{*,2}}} = \sigma_x^* \sqrt{1 + \frac{t^2}{t_x^2}} \quad (3.9)$$

$$\Rightarrow \sigma_y(t) = \sigma_y^* \sqrt{1 + \frac{s^2}{\beta_y^{*,2}}} = \sigma_y^* \sqrt{1 + \frac{t^2}{t_y^2}} \quad (3.10)$$

$$r_{yx} = \frac{\sigma_y^{*,2}}{\sigma_x^{*,2}}, \quad r_{sx} = \frac{\sigma_s^2}{2\sigma_x^{*,2}} \quad (3.11)$$

The Jacobian of the transformation is $J(q, s; u, t) = \frac{2\sigma_x^{*,2}\sigma_s}{u^2}$. Carrying out the transforma-

tion leads to the equations for the general case

$$\begin{aligned} \xi_x = & \frac{\beta_x^* N_p r_e}{2\pi\gamma_e} \left\{ \frac{C_C^2}{(\sigma_x^{*,2})} \int_0^\infty \frac{dt}{\sqrt{2\pi}} \exp\left[-\frac{C_C^2 t^2}{2}\right] \int_0^1 du \exp\left[-\frac{(r_{sx} S_C^2 u t^2)}{1 + u(t/t_x)^2}\right] \right. \\ & \times \left(1 + 2S_C^2 t^2 \left[1 - r_{sx} \frac{u}{1 + u(t/t_x)^2}\right] \right) \left[\frac{1}{(1 + u(t/t_x)^2)^3 (1 + [r_{yx}(1 + (t/t_y)^2) - 1]u)} \right]^{1/2} \\ & - \frac{S_C^2}{\sigma_s^2} \int_0^\infty \frac{dt}{\sqrt{2\pi}} \exp\left[-\frac{C_C^2 t^2}{2}\right] [1 - C_C^2 t^2] \int_0^1 \frac{du}{u} \left(1 - \exp\left[-\frac{r_{sx} S_C^2 u t^2}{1 + u(t/t_y)^2}\right] \right) \\ & \times \left[\frac{1}{(1 + u(t/t_x)^2)(1 + [r_{yx}(1 + (t/t_y)^2) - 1]u)} \right]^{1/2} \Big\} \end{aligned} \quad (3.12)$$

$$\begin{aligned} \xi_y = & \frac{\beta_y^* N_p r_e}{\pi\gamma_e} \frac{1}{(2\sigma_x^{*,2})} \int_0^\infty \frac{dt}{\sqrt{2\pi}} \exp\left[-\frac{C_C^2 t^2}{2}\right] \int_0^1 du \exp\left[-\frac{r_{sx} S_C^2 u t^2}{(1 + u(t/t_x)^2)}\right] \\ & \times \left[\frac{1}{(1 + u(t/t_x)^2)(1 + [r_{yx}(1 + (t/t_y)^2) - 1]u)^3} \right]^{1/2} \end{aligned} \quad (3.13)$$

These expressions involve a finite range of integration (from $0 \rightarrow 1$) over u compared to the infinite range over q in Eq.(3.5) and (3.6). In those equations, the convergence rate is poor and evaluate slowly while the double integrals evaluate quickly in the set Eq.(3.12) and (3.13) above. We note that the second set of terms in Eq.(3.12) proportional to $\frac{S_C^2}{\sigma_s^2}$ are typically very small in the collider applications considered below and can be ignored.

Limiting cases

1. No crossing angle or hourglass effect

In this case $S_C = 0$, $C_C = 1$, so

$$\begin{aligned} \xi_x = & \frac{\beta_y^* N_{+r_e}}{2\pi\gamma_e} t_x \frac{2}{(2\sigma_x^{*,2})} \int_0^\infty \frac{dt}{\sqrt{2\pi}} \exp\left[-\frac{t_x^2 t^2}{2}\right] \int_0^1 du \left[\frac{1}{(1 + (r_{yx} - 1)u)} \right]^{1/2} \\ \xi_y = & \frac{\beta_y^* N_{+r_e}}{\pi\gamma_e} \frac{t_x}{(2\sigma_x^{*,2})} \int_0^\infty \frac{dt}{\sqrt{2\pi}} \exp\left[-\frac{t_x^2 t^2}{2}\right] \int_0^1 du \left[\frac{1}{(1 + (r_{yx} - 1)u)^3} \right]^{1/2} \end{aligned}$$

Using Eqs.(A.1) and (A.2) in the Appendix, we find

$$\xi_x = \frac{\beta_x^* N_{+r_e}}{2\pi\gamma_e} \frac{1}{\sigma_x^*(\sigma_y^* + \sigma_x^*)} \quad (3.14)$$

$$\xi_y = \frac{\beta_y^* N_{+r_e}}{2\pi\gamma_e} \frac{1}{\sigma_y^*(\sigma_y^* + \sigma_x^*)} \quad (3.15)$$

These are the standard expressions for the tune shifts without a crossing angle or hourglass effects.

2. Only a crossing angle

We use the expressions Eq.(3.12) and (3.13), let $t_x, t_y \rightarrow \infty$ and do the integration over t first. Define shorthand variables

$$a^2 = r_{sx} S_C^2, \quad c^2 = \frac{1}{2} C_C^2 \quad (3.16)$$

We use the integration results in Eqs. (A.5) - (A.7) to obtain

$$\begin{aligned} \xi_x &= \frac{\beta_x^* N_{+r_e}}{2\pi\gamma_e} \frac{1}{4\sqrt{2}} \int_0^1 du \left[\frac{1}{(1 + [r_{yx} - 1]u)} \right]^{1/2} \left\{ \frac{2C_C^2}{(2\sigma_x^{*,2})} \frac{2c^2 + 2t_x^2 S_C^2}{(c^2 + a^2 u)^{3/2}} \right. \\ &\quad \left. + \frac{S_C^2}{\sigma_s^2} \frac{1}{u} \frac{2a^2 u}{(c^2 + a^2 u)^{3/2}} \right\} \\ &= \frac{\beta_x^* N_{+r_e}}{2\pi\gamma_e} \frac{1}{C_C^3} \frac{1}{[\sigma_y^* + \sqrt{\sigma_x^{*,2} + T_C^2 \sigma_s^2}] \sqrt{\sigma_x^{*,2} + T_C^2 \sigma_s^2}} \end{aligned} \quad (3.17)$$

$$\begin{aligned} \xi_y &= \frac{\beta_y^* N_{+r_e}}{2\pi\gamma_e} \frac{1}{C_C} \int_0^1 du \frac{1}{\sqrt{(2(\sigma_y^2 - \sigma_x^2)u + 1)^3 [1 + 2(T_C^2 \sigma_s^2)u/(2\sigma_x^2)]}} \\ &= \frac{\beta_y^* N_{+r_e}}{2\pi\gamma_e} \frac{1}{C_C} \frac{1}{\sigma_y(\sigma_y + \sqrt{\sigma_x^2 + T_C^2 \sigma_s^2})} \end{aligned} \quad (3.18)$$

These expressions can be obtained from the equations (3.14), (3.15) by replacing the transverse beam size σ_x in the crossing plane by the effective beam size $\sqrt{\sigma_x^2 + T_C^2 \sigma_s^2}$ and including the factors $1/C_C^3$ in ξ_x , $1/C_C$ in ξ_y which are ~ 1 for typical crossing angles.

3. Only the hourglass, no crossing angle

Setting $C_C = 1, S_C = 0, = 1$ in the general forms Eq.(3.12), and (3.13)

$$\begin{aligned} \xi_x &= \frac{\beta_x^* N_{+r_e}}{2\pi\gamma_e} \left\{ \frac{2}{(2\sigma_x^{*,2})} \int_0^\infty \frac{dt}{\sqrt{2\pi}} \exp\left[-\frac{t^2}{2}\right] \right. \\ &\quad \left. \times \int_0^1 du \left[\frac{1}{(1 + ut^2/t_x^2)^3 (1 + [r_{yx}(1 + t^2/t_y^2) - 1]u)} \right]^{1/2} \right\} \\ \xi_y &= \frac{\beta_y^* N_{+r_e}}{\pi\gamma_e} \frac{1}{(2\sigma_x^{*,2})} \int_0^\infty \frac{dt}{\sqrt{2\pi}} \exp\left[-\frac{t^2}{2}\right] \\ &\quad \times \int_0^1 du \left[\frac{1}{(1 + u(t/t_x)^2)(1 + [r_{yx}(1 + (t/t_y)^2) - 1]u)^3} \right]^{1/2} \end{aligned}$$

Integrating over u yields the expressions

$$\xi_x = \frac{\beta_x^* N_{+r_e}}{\pi\gamma_e \sigma_x^{*,2}} \int_0^\infty \frac{dt}{\sqrt{2\pi}} \exp[-t^2/2] \frac{1}{\sqrt{(1 + \frac{t^2}{t_x^2})} \left[\sqrt{1 + \frac{t^2}{t_x^2}} + \frac{\sigma_y^*}{\sigma_x^*} \sqrt{1 + \frac{t^2}{t_y^2}} \right]} \quad (3.19)$$

$$\xi_y = \frac{\beta_y^* N_{+r_e}}{2\pi\gamma_e \sigma_y^{*,2}} \int_0^\infty \frac{dt}{\sqrt{2\pi}} \exp[-t^2/2] \frac{1}{\sqrt{(1 + \frac{t^2}{t_y^2})} \left[\sqrt{1 + \frac{t^2}{t_y^2}} + \frac{\sigma_x^*}{\sigma_y^*} \sqrt{1 + \frac{t^2}{t_x^2}} \right]} \quad (3.20)$$

These agree with Eq.(3.4) (evaluated at $s = 0$) in[4].

4. Flat beams

Here we consider the limit $t_x \rightarrow \infty$ in the general expressions in Eqs (3.12), (3.13). Interchanging the integrations and we drop the second set of terms $\propto S_C^2$ in ξ_x that are negligibly small

$$\begin{aligned} \xi_x &= \frac{\beta_x^* N_{+r_e}}{2\pi\gamma_e} \frac{2C_C^2}{(2\sigma_x^{*,2})} \int_0^1 du \int_0^\infty \frac{dt}{\sqrt{2\pi}} \exp[-t^2(\frac{1}{2}C_C^2 + r_{sx}S_C^2u)] \\ &\quad \times (1 + 2S_C^2t^2[1 - r_{sx}u]) \left[\frac{1}{(1 + (r_{yx} - 1)u + r_{yx}ut^2/t_y^2)} \right]^{1/2} \end{aligned} \quad (3.21)$$

$$\begin{aligned} \xi_y &= \frac{\beta_y^* N_{+r_e}}{\pi\gamma_e} \frac{1}{(2\sigma_x^{*,2})} \int_0^1 \int_0^\infty \frac{dt}{\sqrt{2\pi}} \exp[-t^2(\frac{1}{2}C_C^2 + r_{sx}S_C^2u)] \\ &\quad \times \left[\frac{1}{(1 + (r_{yx} - 1)u + r_{yx}ut^2/t_y^2)} \right]^{3/2} \end{aligned} \quad (3.22)$$

The integrations over t can be done and expressed in terms of confluent hypergeometric function U and the Bessel function K_0 . Using integration results in the Appendix and identifying the coefficients in the equations (A.8) and (A.9)

$$\begin{aligned} a^2 &= \frac{1}{2}C_C^2 + r_{sx}S_C^2u, \quad (\text{Note } u \geq 0), \quad b = 2S_C^2[1 - r_{sx}u] \\ c &= 1 + (r_{yx} - 1)u, \quad d = r_{yx}u/t_y^2 \end{aligned}$$

leads to the expressions for the tune shifts in the flat beam limit as

$$\begin{aligned} \xi_x &= \frac{\beta_x^* N_{+r_e}}{2\pi\gamma_e} \frac{2C_C^2}{2\sigma_x^{*,2}\sqrt{2\pi}} \int_0^1 du \frac{1}{4(\frac{1}{2}C_C^2 + r_{sx}S_C^2u)\sqrt{r_{yx}u/t_y^2}} \\ &\quad \left\{ (C_C^2 + 2r_{sx}S_C^2u) \exp[\arg] K_0(\arg) + \sqrt{\pi} 2S_C^2[1 - r_{sx}u] U(\frac{1}{2}, 0, 2 \arg) \right\} \end{aligned} \quad (3.23)$$

$$\xi_y = \frac{\beta_y^* N_{+r_e}}{\pi\gamma_e} \frac{1}{2\sqrt{2}\sigma_x^{*,2}} \int_0^1 du \frac{1}{2(1 + (r_{yx} - 1)u)\sqrt{r_{yx}u/t_y^2}} U(1/2, 0, 2 \arg) \quad (3.24)$$

$$\arg = \frac{(\frac{1}{2}C_C^2 + r_{sx}S_C^2u)(1 + (r_{yx} - 1)u)}{2r_{yx}u/t_y^2} \quad (3.25)$$

This in principle, leaves the integration over u to be evaluated numerically. While the integrations over the hypergeometric function U in both ξ_x, ξ_y converge rapidly for typical parameter values, the integration over the Bessel function K_0 in ξ_x is poorly convergent. We found it more convenient to use the double integration in Eq.(3.21) to evaluate ξ_x and the single integration in Eq.(3.24) to evaluate ξ_y . In the following sections, we have used the exact expressions for the luminosity and the beam-beam tune shifts for both the Fermi site filler and the FCC-ee but in both cases, the flat beam expressions are very good approximations.

4 Higgs Factory Site Filler

Beam energy [GeV]	120
Circumference [km]	16.0
Bunch intensity	8.34×10^{11}
Number of bunches	2
Emittance x [nm] / y [pm]	0. /
β_x^*/β_y^* [m]	0.2 / 0.001
σ_z [mm]	2.9
Nominal crossing angle [mrad]	0

Table 1: Parameters of the Fermilab site filler

Table 1 shows the parameters in the very preliminary design of a Higgs factory based at Fermilab [6]. The bunch length in the table above is the equilibrium value with only synchrotron radiation emitted in the arcs and does not include the beamsstrahlung effect that would increase the bunch length. Hence, the hourglass effects for the site filler are a slight underestimate of the exact values. Table 2 shows the luminosity and the beam-beam tune shifts with and without the hourglass effect.

	Without hourglass	With hourglass
Luminosity [$\text{cm}^{-2}\text{s}^{-1}$]	1.56×10^{34}	9.5×10^{33}
Beam-beam tune shift $\xi_x, / \xi_y$	0.00849 / 0.1197	0.00845 / 0.0614

Table 2: Luminosity and beam-beam tune shifts in the Fermi site filler with the parameters shown in Table 1.

The first plot in Fig.1 show the luminosity as a function of the so called Piwinski angle parameter $\Phi = \tan(\theta_C/2)\sigma_z/\sigma_x^*$ for four values of β_x^* . This shows that the luminosity is relatively flat upto $\Phi \sim 0.5$ which corresponds to $\theta_C = 21$ mrad or 69 times the beam divergence, a relatively large value. The second plot shows the luminosity as function of Φ and β_x^* over the ranges $0 \leq \Phi \leq 5$ and $0.01[m] \leq \beta_x^* \leq 0.20[m]$ respectively. This plot shows that the luminosity varies slowly as a function of Φ over $0 \leq \Phi \leq 0.5$, more rapidly from $0.5 \leq \Phi \leq 2$ and then is relatively flat over $2 \leq \Phi \leq 5$. Decreasing β_x^* from 0.2 m to 0.01 m increases the luminosity to nearly $4 \times 10^{34} \text{ cm}^{-2} \text{ s}^{-1}$ for $0 \leq \Phi \leq 0.5$. However, the vertical tune shift at these parameters is very large at ~ 0.25 , as the next figure shows. The top plot in Fig. 2 shows the vertical tune shift as a function of β_x^* at constant $\Phi = 0.5$ for different cases showing the relative impact of the crossing angle and hourglass effects. It is clear that the hourglass effect is dominant in determining the vertical tune shift. The bottom plots in this figure show the horizontal and vertical tune shifts as functions of β_x^* and Φ with both effects included. The horizontal tune shift ξ_x varies more strongly with the crossing angle and is mostly independent of β_x^* . The vertical tune shift on the other hand, varies strongly with β_x^* and slowly with Φ . Assuming that tune shifts of ~ 0.12 are

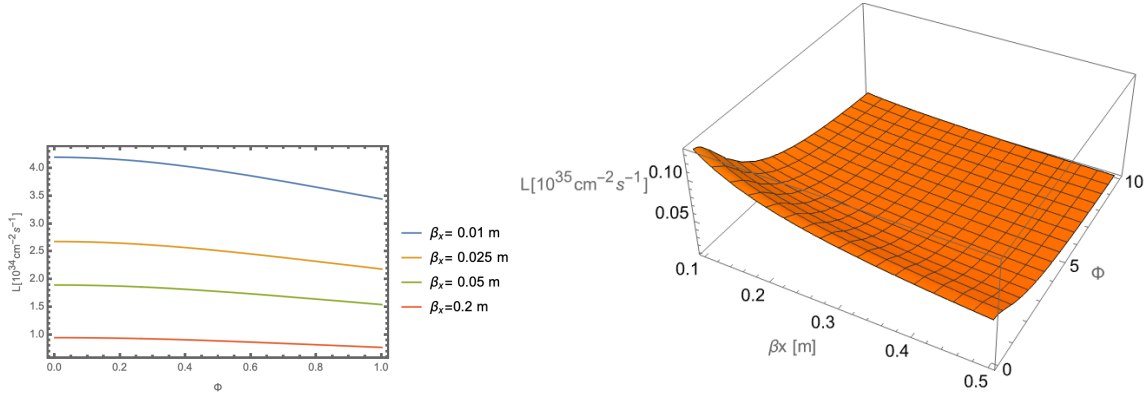


Figure 1: (Left): Luminosity as a function of the Piwinski angle Φ for four values of β_x^* . (Right): Luminosity as a function of Φ and β_x^* . β_y^* is constant at 1mm in both figures.

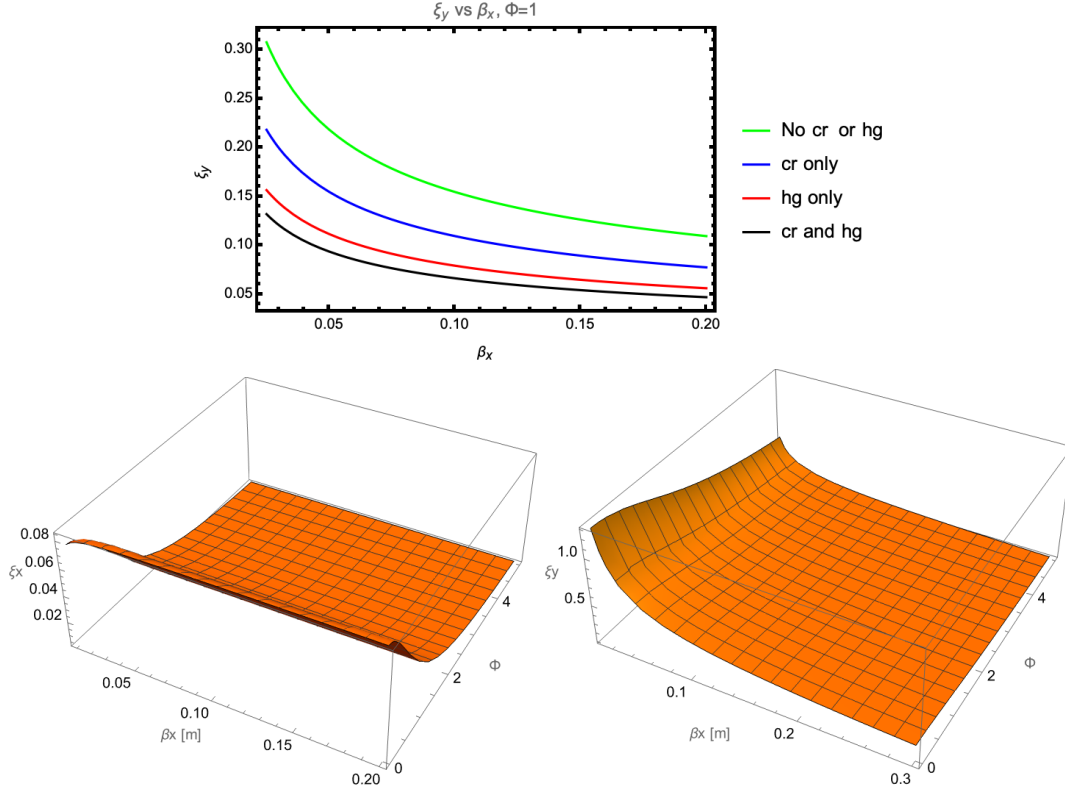


Figure 2: Top: Vertical beam-beam tune shift ξ_y as a function of β_x^* for different cases; no crossing angle (Cr) and no hourglass (Hg), only the crossing angle, only the hourglass and with both effects. $\Phi = 0.5$ in all cases. Bottom: Horizontal and vertical tune shifts as functions of Φ and β_x^* . β_y^* is constant at 1mm in all figures.

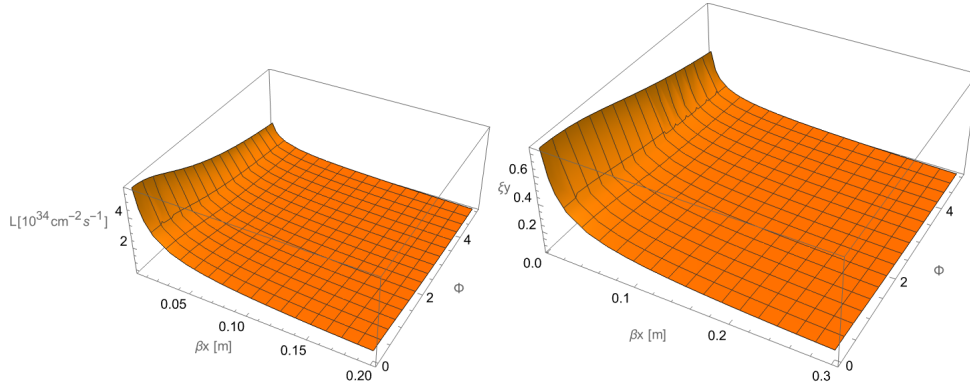


Figure 3: Luminosity and ξ_y as functions of β_x^* and Φ at $\beta_y^* = 0.5\text{mm}$.

dynamically sustainable and the increased chromaticity can be corrected, this suggests that β_x^* could be lowered to values in the range $0.025 \leq \beta_x^* \leq 0.05\text{m}$ with $\beta_y^* = 0.001\text{ m}$. These would increase luminosity to the range $(2 - 2.5) \times 10^{34} \text{ cm}^{-2}\text{s}^{-1}$. We can be more aggressive by lowering β_y^* further. The plots in Fig. 3 show that with $\beta_x^* \leq 0.01\text{ m}$, $\beta_y^* = 0.0005\text{m}$, $\Phi < 2$, the vertical beam-beam tune shift $\xi_y \leq 0.14$ and the luminosity increases to $\sim 4 \times 10^{34} \text{ cm}^{-2}\text{s}^{-1}$. The major challenge at these parameters will be to control the linear and non-linear IR chromaticities at these values of β_x^*, β_y^* .

5 FCC-ee collider

We apply the theory developed above to the FCC e^+e^- collider. The required parameters are shown in Table 3 taken from [2]. The bunch length in Table 3 has been calculated with

Beam energy [GeV]	120
Circumference [km]	97.75
Bunch intensity	1.8×10^{11}
Number of bunches	328
Emittance x [nm] / y [pm]	0.63 / 1.3
β_x^* / β_y^* [m]	0.3 / 0.001
σ_z [mm]	5.3
Crossing angle (mrad) / Piwinski angle Φ	30 / 5.8

Table 3: Parameters of the FCC-ee

	No Cr or Hg	Hg only	Cr only	Hg and Cr	FCC study
$\mathcal{L} [10^{34} \text{ cm}^{-2} \text{ s}^{-1}]$	52	23	8.9	7.8	8.5
ξ_x / ξ_y	0.544 / 0.692	0.539 / 0.253	0.0158 / 0.118	0.0159 / 0.096	0.016 / 0.118

Table 4: Luminosity and beam-beam tune shifts at the FCC parameter values used in the FCC study.

beamsstrahlung effects included, according to reference [2].

Table 4 shows the luminosity and beam-beam tuneshifts calculated with different conditions in the several columns: (a) No crossing angle or hourglass, (b) hourglass only, (c) crossing angle only, (d) both hourglass and crossing angle. These are compared with the values found in the FCC study [2]. We find that our results with only the crossing angle are close to the FCC study values but our values with both effects are lower, especially the vertical beam-beam tune shift which is more than 20% lower. This is expected since $\beta_y^* \ll \sigma_z$ while $\beta_x^* > \sigma_z$.

The left plot in Fig. 4 shows the luminosity correction factor R_L from Eq. (2.12) as a function of the Piwinski angle Φ at nominal values of β_x^*, β_y^* for the cases with only the hourglass factor, only the crossing angle and with both effects included. For the FCC parameters, the reduction due to the crossing angle exceeds the reduction due to the hourglass factor when $\Phi > 2$. The right plot shows the luminosity as a function of Φ for different values of β_x^* . We observe, for example, that the luminosity at say $\beta_x^* = 0.05 \text{ m}$ is in the range $1.2 \leq \mathcal{L} [\text{cm}^{-2} \text{ s}^{-1}] \leq 6 \times 10^{35}$ while the range at the nominal $\beta_x^* = 0.3 \text{ m}$ is $0.49 \leq \mathcal{L} [\text{cm}^{-2} \text{ s}^{-1}] \leq 2.5 \times 10^{35}$. The increase in luminosity at lower β_x^* decreases at larger crossing angles.

The top plots in Fig. 5 show ξ_y as a function of Φ with or without the two effects (left) and for different values of β_x^* . The left plot shows that at $\beta_x^* = 0.3$ and at zero crossing angle, $\xi_y = 0.67$ and 0.22 without and with the hourglass effect respectively. This value drops to 0.096 at the nominal crossing angle. The hourglass effect therefore significantly reduces

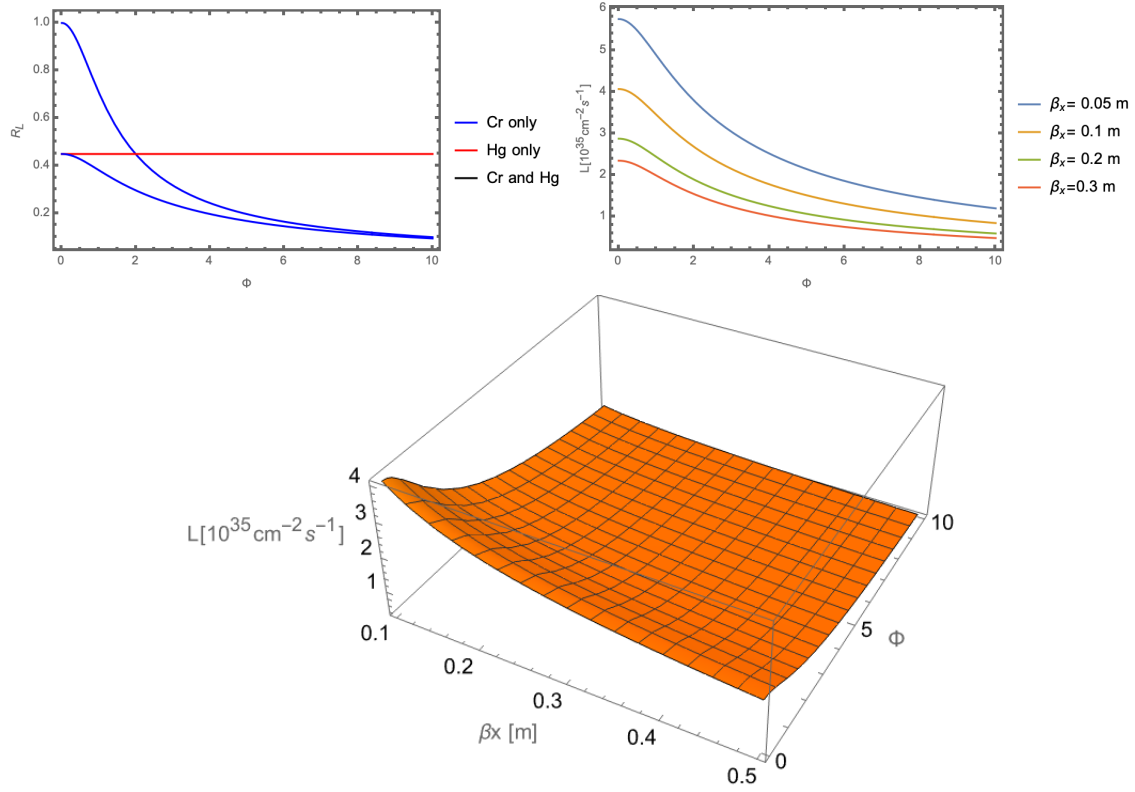


Figure 4: Top Left: The correction factor R_L vs Φ for the cases (a) only the crossing angle (Cr), (b) only the hourglass (hg), and (c) both crossing angle and the hourglass. Top right: Luminosity as a function of Φ for different values of β_x^* with both effects. Bottom: Luminosity as a function of β_x^* and Φ .

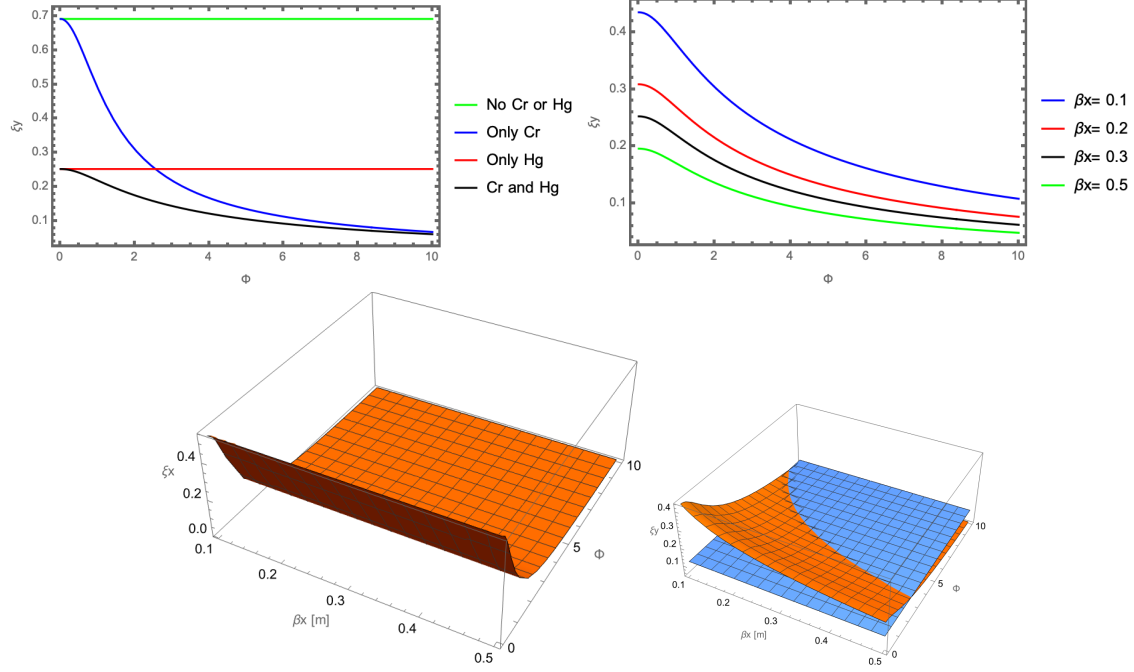


Figure 5: Top row : Vertical beam-beam parameter as a function of Φ at $\beta_x^* = 0.3$ m for different conditions (left) and different β_x^* values (right). Bottom: ξ_x (left), and ξ_y (right) as functions of β_x^* and Φ . In the right figure is also shown the plane (in blue) at $\xi_y = 0.12$ intersecting the function $\xi_y(\Phi, \beta_x^*)$.

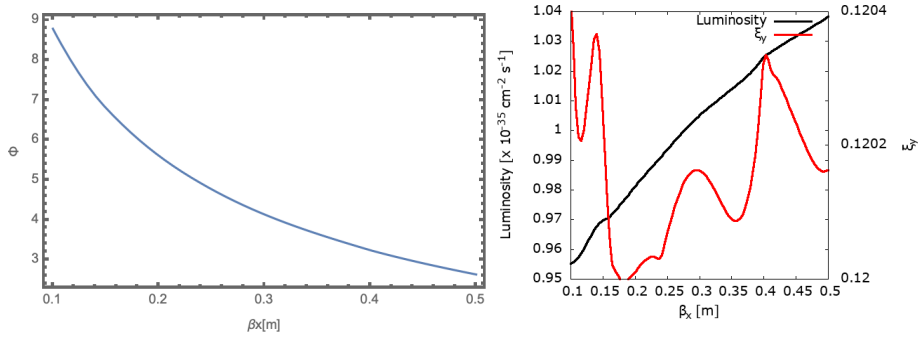


Figure 6: Top: Φ as a function of β_x at a constant value of $\xi_y = 0.12$. Bottom: Luminosity (left vertical axis) and ξ_y (right vertical axis) as functions of β_x^* with the crossing angle determined by the top figure.

the vertical beam-beam tunes shift. The right plot shows, among other observations, that ξ_y is more sensitive to the value of β_x^* at smaller Φ than at larger Φ . The bottom plots in Fig. 5 show ξ_x, ξ_y as functions of β_x^*, Φ . As expected, ξ_x is insensitive to β_x^* and falls sharply with increasing Φ . The right plot shows $\xi_y(\beta_x^*, \Phi)$ intersected with a planar surface (in blue) at $\xi_y = 0.12$, assumed to be a target value. The intersection of the two surfaces is a curve Φ as a function of β_x^* along which $\xi_y = 0.12$. The left plot in Fig. 6 shows this curve explicitly, calculated numerically. Assuming that the bunch intensity is kept constant, this curve can be used to find the values of β_x^*, Φ that maximize the luminosity while keeping ξ_y constant. The right plot in this figure shows the luminosity (in black) is $\mathcal{L} \sim 10^{35} \text{ cm}^{-2} \text{ s}^{-1}$ over the range $0.1 \leq \beta_x^* \leq 0.5$ with the corresponding Φ found from the left plot. Compared to the luminosity $\mathcal{L} = 0.79 \times 10^{34} \text{ cm}^{-2} \text{ s}^{-1}$, this represents a 26% increase in luminosity. This is comparable to the 25% luminosity increase achievable by increasing the bunch intensity to increase ξ_y from 0.096 to 0.12 at the nominal β_x^* and Φ . However the first method increases β_x^* from 0.3 to 0.5 and lowers the crossing angle from 30 mrad to ~ 15 mrad. This has additional benefits of keeping the synchrotron radiation power constant, lowering the IR chromaticity and reducing aperture restrictions, and other effects from the smaller crossing angle and avoids potential problems at higher currents.

6 Conclusions

We developed exact expressions for the luminosity and beam-beam tunes shifts with both crossing angle and hourglass effects. We showed that the expressions reduce to known expressions in the limit that one or the other effect is absent.

As mentioned earlier, the Fermi site filler design is very preliminary and detailed studies of the dynamics with beam-beam interactions need to be done. The nominal design has one Interaction Point, a zero crossing angle and achieves a peak luminosity $\sim 10^{34} \text{ cm}^{-2} \text{ s}^{-1}$. We find that with a crossing angle around 21 mrad, $0.025 \leq \beta_x^* \leq 0.05 \text{ m}$ would increase luminosity to the range $(2 - 2.5) \times 10^{34} \text{ cm}^{-2} \text{ s}^{-1}$ with ξ_y nearly constant at 0.12. Since there is only one IP, it is possible that ξ_y could be increased from this value with an accompanying increase in the luminosity.

The FCC-ee design is considerably more advanced. Applying the theory developed in this report, we have the following observations:

- The crossing angle and the hourglass effect together reduce the luminosity and vertical beam-beam tunes shift compared to the values with the crossing angle alone. With both effects, the luminosity is $7.8 \times 10^{34} \text{ cm}^{-2} \text{ s}^{-1}$ compared to $8.9 \times 10^{34} \text{ cm}^{-2} \text{ s}^{-1}$ with only the crossing angle. The values with only the crossing angle are close to those obtained in the FCC study. More significantly, the values of ξ_y under the same conditions are 0.096 and 0.118 respectively.
- Assuming a target value of $\xi_y = 0.12$, this suggests that the luminosity can be increased from the present value.
- We find the luminosity can be increased by $\sim 25\%$ to $1 \times 10^{35} \text{ cm}^{-2} \text{ s}^{-1}$ by simultaneously decreasing the crossing angle to $\theta_C \sim 15$ mrad and increasing β_x^* to 0.5 m

while keeping the vertical tuneshift at 0.12. This would be better than the alternative method of increasing the bunch intensity while keeping the nominal values $\theta_C = 30$ mrad and $\beta_x^* = 0.3\text{m}$.

Acknowledgments

Fermilab is operated by Fermi Research Alliance LLC under DOE contract No. DE-AC02CH11359.

References

- [1] K. Akai et al, *Super KEKB Collider*, Nucl.Instrum.Meth. **A 907**, 188 (2018)
- [2] A. Abada et al, *FCC-ee: The Lepton Collider*, Eur. Phys. J. Special Topics **228**, 261–623 (2019)
- [3] M.A. Furman and M.S. Zisman, *Luminosity* in Handbook of Accelerator Physics and Engineering, editors: A.W. Chao, M. Tigner and F. Zimmermann
- [4] M.A. Furman, *The hourglass reduction factor for asymmetric colliders*, SLAC-ABC-81
- [5] K. Hirata, *Analysis of beam-beam interactions with a large crossing angle*, Phys. Rev. Lett. , **74**, 2228 (1995)
- [6] P.C. Bhat et al, *Future collider options for the US*, e-Print: 2203.08088 (on arxiv)

7 Appendix: Integration results

The integrations for the tune shift without crossing angle or hourglass effects use

$$\int_0^1 du \left[\frac{1}{(1 + (r_{yx} - 1)u)} \right]^{1/2} = 2 \frac{\sigma_x^*}{\sigma_y^* + \sigma_x^*} \quad (\text{A.1})$$

$$\int_0^1 du \left[\frac{1}{(1 + (r_{yx} - 1)u)^3} \right]^{1/2} = 2 \frac{\sigma_x^{*,2}}{\sigma_y^*(\sigma_y^* + \sigma_x^*)} \quad (\text{A.2})$$

The integrations for the tune shifts with crossing angle only use the results below

$$\int_0^\infty \frac{dt}{\sqrt{2\pi}} \exp[-a^2 t^2](1 + bt^2) = \frac{1}{4\sqrt{2}} \frac{2a^2 + b}{a^3} \quad (\text{A.3})$$

$$\int_0^1 \frac{dz}{\sqrt{(1 + U's)(1 + Cz)^3}} = \frac{2}{(\sqrt{A+1} + \sqrt{C+1})\sqrt{1+C}} \quad (\text{A.4})$$

Using these results, the integrals over t for ξ_x, ξ_y yield

$$\int_0^\infty \frac{dt}{\sqrt{2\pi}} \exp[-(c^2 + a^2 u)t^2/t_x^2] [1 + 2S_C^2(1 - r_{sx}u)t^2/t_x^2] = \frac{1}{4\sqrt{2}} t_x \frac{2c^2 + 2S_C^2}{(c^2 + a^2 u)^{3/2}} \quad (\text{A.5})$$

$$\int_0^\infty \frac{dt}{\sqrt{2\pi}} \exp[-c_e^2 t^2] [1 - 2c^2 t^2] = 0 \quad (\text{A.6})$$

$$\int_0^\infty \frac{dt}{\sqrt{2\pi}} \exp[-(c^2 + a^2 u)t^2] [1 - 2c^2 t^2] = \frac{1}{4\sqrt{2}} \frac{2a^2 u}{(c^2 + a^2 u)^{3/2}} \quad (\text{A.7})$$

Beam-beam tune shifts for flat beams

$$\int_0^\infty dt \exp[-a^2 t^2] \frac{1 + bt^2}{\sqrt{c + dt^2}} = \frac{1}{4a^2 \sqrt{d}} \left\{ 2a^2 \exp[a^2 c/(2d)] K_0\left(\frac{a^2 c}{2d}\right) + b\sqrt{\pi} U\left(\frac{1}{2}, 0, \frac{a^2 c}{d}\right) \right\} \quad (\text{A.8})$$

$$\int_0^\infty dt \exp[-a^2 t^2] \frac{1}{(c + dt^2)^{3/2}} = \frac{\sqrt{\pi}}{2c\sqrt{d}} U(1/2, 0, \frac{a^2 c}{d}) \quad (\text{A.9})$$

where $U(\frac{1}{2}, 0, x)$ is the confluent geometric function which, to leading order, decays as $1/\sqrt{x}$.